1240 nm diamond Raman laser operating near the quantum limit

Alexander Sabella,[1,2,*] James A. Piper,[2] and Richard P. Mildren[2]

[1]*Defence Science and Technology Organisation, Edinburgh, South Australia, 5111, Australia*

[2]*MQ Photonics Research Centre, Macquarie University, Sydney, New South Wales, 2109, Australia*

**Corresponding author: alexander.sabella@dsto.defence.gov.au*

Received August 20, 2010; revised October 18, 2010; accepted October 22, 2010;
posted October 26, 2010 (Doc. ID 133743); published November 18, 2010

An external-cavity diamond Raman laser generating up to 2.0 W at 1240 nm from 3.3 W of 1064 nm pump power is investigated as a function of pump polarization direction. The maximum conversion efficiency was 61%, and the slope efficiency of 84% closely approaches the quantum limit of 85.8%. The lowest threshold for Raman lasing is achieved for pump polarization parallel to the ⟨111⟩ axis, which we show is consistent with theory.

OCIS codes: 140.3550, 140.3580, 160.4330, 190.5650.

Diamond has very high Raman gain and can be synthesized with low impurities and defects [1]. Its exceptional thermal conductivity, high damage threshold, and broad transparency provide excellent prospects for a range of efficient, compact, and high-power laser devices. The 1333 cm^{-1} Raman frequency, which is notably larger than other Raman crystals (<1100 cm^{-1}), provides a first Stokes wavelength of 1240 nm for 1064 nm pumping, which is interesting for a range of medical and defense applications, and is also the first step toward the 1485 nm second Stokes wavelength in the "eye-safe" region. However, diamond Raman laser (DRL) development is immature compared to other Raman crystals and, as far as we are aware, highly efficient performance in the IR has not yet been obtained.

Infrared DRL studies to date have focused on designs in which the diamond is placed within the pump laser cavity. A 1240 nm microchip DRL was first reported in 2005 [2], but few details are available. Recently [3], an intracavity DRL based on a 3.3-mm-long diamond crystal placed inside a *Q*-switched Nd:YVO_4 laser resonator was reported, but the conversion efficiency from the diode pump was limited by round-trip losses to 4% (cf. >20% diode to first Stokes conversion has been achieved with other Raman crystals, e.g., [4]). The external cavity configuration has the practical advantage of being easily adapted to existing pump laser systems, while it also allows straightforward determination of the efficiency of the Raman conversion step. Conversion of 1064 nm using other Raman crystals in external cavities is well documented, with conversion efficiencies from 1064 nm to the first Stokes in barium nitrate of 60% [5] and in barium tungstate of 62.6% [6]. In diamond, an external-cavity laser pumped in the visible (532 nm) has been shown to have efficiency of up to 65%, slightly higher than the reported efficiencies of other materials despite the slightly higher quantum defect [7]. An external-cavity DRL is thus promising as an efficient wavelength converter in the IR.

In this Letter, we report an external-cavity DRL with up to 61% conversion efficiency to the first Stokes and with a slope efficiency very close to the 85.8% first Stokes quantum efficiency. As in previous extracavity DRL experiments [7], the diamond was cut for propagation along the ⟨110⟩ direction. However, in this work we used antireflection (AR) coatings on the end facets, rather than Brewster-angled facets, to allow performance to be investigated as a function of pump polarization angle. We show for the first time, to the best of our knowledge, that the laser threshold is minimized for pump polarization parallel to the ⟨111⟩ axes, in accordance with the crystal polarizability.

The DRL used a 6.9-mm-long AR coated (reflectivity <0.4% per surface at 1240 nm), rectangular, Type IIa single diamond crystal grown by chemical vapor deposition (CVD) (Element Six, UK). The birefringence of the central portion was $\Delta n < 1 \times 10^{-6}$, measured using birefringence microscopy (Metripol). The DRL was pumped by a linearly polarized, 4.5 W (0.9 mJ), *Q*-switched Nd:YAG laser with 10 ns pulses at 5 kHz. It had a beam quality factor of $M^2 < 1.5$ and a power stability of ±1%. An isolator was used to prevent backreflections from the Raman cavity. The pump amplitude was varied while maintaining a consistent pulse shape by rotating a half-wave plate prior to the isolator. A second half-wave plate after the isolator was used to vary the pump polarization angle with respect to the diamond crystal axis. The pump beam was focused into the Raman cavity using a 100 mm focal length singlet lens. The 115 μm pump spot size, which significantly underfilled the cavity mode (~360 μm at 1240 nm), was experimentally found to offer the lowest threshold without damaging the crystal in the range of investigated input powers. The slope efficiency was essentially independent of pump spot size for values smaller than the cavity mode size. The input and output coupler mirrors were placed approximately 2 mm from the diamond crystal. The flat input coupler was 98% transparent at 1064 nm, highly reflective (>99.9%) at 1240 nm, and 50% reflective at the second Stokes wavelength of 1485 nm. The output coupler had a 1000 mm radius of curvature (ROC) and reflectivities of >99.9%, 50%, and 3% at the pump, first, and second Stokes wavelengths, respectively. Power measurements were made using a Newport 818P-010-12 head (±0.5% repeatability). The pump input powers reported are corrected for the loss through the input coupler.

The Raman lasing threshold as a function of pump polarization is shown in Fig. 1. Minima in thresholds occur when the pump polarization is approximately ±55° from the [100] crystal direction (axes are defined in Fig. 2).

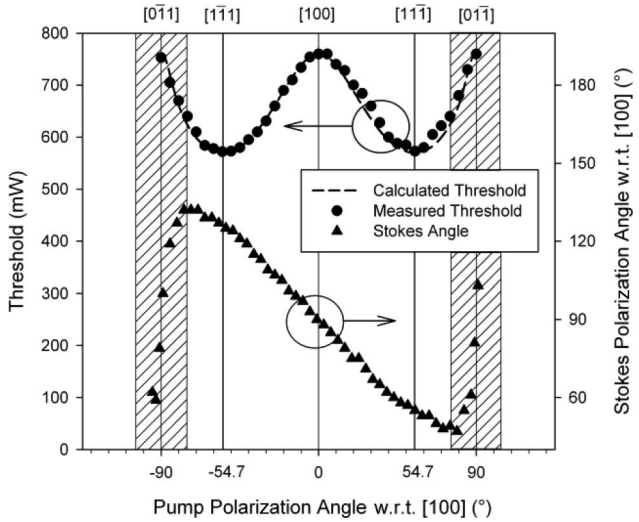

Fig. 1. First Stokes threshold and polarization angle for varying pump polarization angle. The shaded regions represent areas where two orthogonal polarizations are above threshold for 1.4 W of pump.

Maximum thresholds are observed when the pump polarization is aligned with the [01$\bar{1}$] and [100] axes. The threshold behavior is consistent with the Raman polarizability of diamond as a function of the pump polarization direction. The scattering probability, and thus the Raman gain, can be deduced from the three Raman scattering tensors corresponding to the triply degenerate F_{2g} vibrational modes of diamond's O_h point group. For spontaneous Raman scattering, the relative scattered intensity [8] is given by

$$I_S \propto |e_S^T R_1 e_p|^2 + |e_S^T R_2 e_p|^2 + |e_S^T R_3 e_p|^2. \quad (1)$$

e_p and e_s are unit vectors aligned with the pump and Stokes polarization, respectively. R_{1-3} are the scattering tensors, which are given in [9] for the orientation described in Fig. 2. At a pump polarization angle of 54.7° to [100], the calculated scattered intensity peaks at a value 1.33 times that for 0° or 90°. Given that the Raman gain coefficient is proportional to the scattered Stokes intensity [10], the lasing threshold is expected to be reduced by a factor of 1.33. By inverting and scaling the calculated relative scattering intensity values, an excellent match is obtained with the measured lasing thresholds (see Fig. 1).

The significance of the 54.7° polarization angle is apparent when viewing the structure of the crystal lattice along the [011] direction of laser propagation, as shown in Fig. 2. The polarization direction is parallel to the covalent bonds directed along the ⟨111⟩ axes that connect the two interpenetrating face centered cubic lattices that rigidly vibrate against each other at the frequency of the first order Raman mode [11]. When the pump electric field is aligned with these bonds, the change in polarizability and the Raman gain coefficient are maximal. An analysis of the Raman tensors over all angles suggests this angle provides the maximum gain coefficient available in diamond for linearly polarized pumping.

To date, investigations of Raman lasers and stimulated Raman scattering along with accompanying measurements of the Raman gain coefficient, g, are mostly for pump polarizations along the ⟨100⟩ or ⟨110⟩ directions.

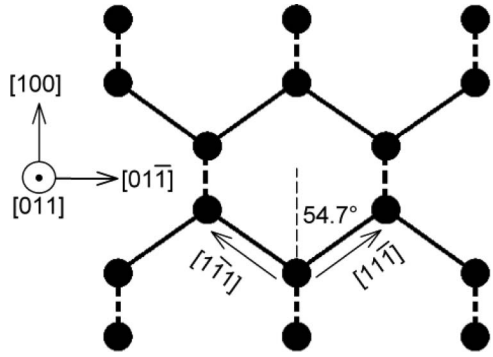

Fig. 2. Diamond crystal lattice as viewed along the direction of laser propagation. Dashed lines represent bonds not contained within a plane parallel to the page.

The most recently published direct measurement of g for single crystal CVD diamond, >12.5 cm/GW at 1064 nm [12], appears to be performed for a probe laser propagating along ⟨100⟩ (assuming the growth direction is ⟨100⟩). As a result, the probe polarization was in the {100} plane and thus at least 35° from the ⟨111⟩ direction. This suggests g for pump polarization along ⟨111⟩ is >16.6 cm/GW.

Figure 1 also shows the dependence of Stokes output polarization on input polarization for input power twice above threshold. When the pump polarization is aligned with [01$\bar{1}$], there are two orthogonal Raman modes of similar magnitude. Since they compete for available pump power and the Raman intensity builds up from noise, the ratio of the two modes in each pulse varies from pulse to pulse. The time-averaged Stokes output thus has an elliptical power distribution when measured through a polarization analyzer. The data points within the shaded region of Fig. 1 are the major axis angle of the ellipse. The ellipticity increases as the pump polarization angle deviates from [01$\bar{1}$], and once the angle is greater than 10°–15° (pump power dependent), one mode dominates and the Stokes output polarization is linear. It should be noted that the only case where the pump and Stokes polarization angles are equal is for pump polarizations along ⟨111⟩ directions.

We compare performance of the Raman laser for input polarizations along the [100] and [11$\bar{1}$] directions as shown in Fig. 3. For [100], higher threshold for first and second Stokes are observed, consistent with the lower gain at the pump polarization and the perpendicularly polarized first Stokes polarization. Both pumping polarizations lead to similar maximum conversion efficiencies to the first Stokes of 61% and total Stokes of 65%. Prior to the onset of second Stokes output, the slope efficiency is 84% and closely approaches the first Stokes quantum efficiency of 85.8%. In terms of photon conversion to a single Stokes order, the efficiency is 71%, which we believe is the highest for any crystalline Raman laser yet reported.

To provide further evidence of the near quantum limited operation, the double-passed residual pump power was recorded, as also plotted in Fig. 3. It was measured from the reflection off a slightly tilted AR coated window placed prior to the DRL cavity. The powers measured below threshold were used to scale the readings. Below threshold, the residual pump increases linearly with input power, as expected. Above threshold, the residual

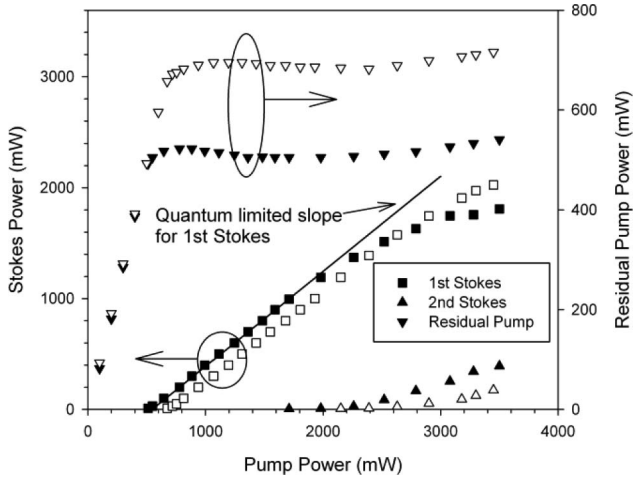

Fig. 3. Stokes powers and residual pump power for increasing pump input. Filled markers are for pump polarization aligned with $[11\bar{1}]$. Hollow markers are for pump aligned with [100].

pump power rapidly rolls over and remains approximately constant thereafter. In fact, we systematically observe a slight decrease in the measured residual pump power for input powers up to 2–3 times threshold. This indicates that each additional pump photon leads to the generation of fractionally more than one Stokes output photon on average. We attribute this phenomenon to an increasing temporal overlap in the Stokes and pump pulses as the input pulse energy is increased. Measurements of the temporal pulse dynamics show that, near threshold, the peak of the Stokes pulse is as short as a few nanoseconds in duration and occurs approximately 2–3 ns after the peak of the pump pulse. As pump power is increased, the Stokes pulse broadens up to 8 ns and the peak becomes aligned with the peak of the pump pulse. Since the rate of pump depletion and first Stokes generation depend on both the pump and Stokes intensity, a greater fraction of the pump pulse is above threshold at higher pulse energies. Despite this effect, the measured slope efficiency is slightly less than the quantum efficiency owing to minor parasitic losses at the pump and Stokes wavelengths. Once the second Stokes threshold is reached, partial conversion of first Stokes to 1485 nm hinders subsequent conversion of the pump to the first Stokes. This is observed by a small positive slope in the residual pump signal.

For applications, it is often desirable to obtain efficient performance at a selected Stokes order. It is clear from Fig. 3 that, to maintain near quantum limited first Stokes slope efficiency, second Stokes operation must be suppressed. A straightforward method to suppress the second Stokes is to minimize the input and output mirror reflectivities at 1485 nm. In our case, there is scope to reduce the reflectivity of the input coupler. We have also found that second Stokes can be further suppressed by increasing the cavity mirror ROC, presumably owing to a reduction in the intracavity first Stokes power density. For example, by increasing the output coupler ROC from 100 to 1000 mm, an additional 0.2 W of 1240 nm power is achieved before the second Stokes threshold is reached (the corresponding increase in first Stokes threshold is only a few tens of milliwatts). Alternatively, the laser cavity can be designed for maximum second Stokes power in order to develop an efficient pulsed laser operating in the eye-safe region.

R. P. M. acknowledges the support of an Australian Research Council Future Fellowship (project number FT0990622).

References

1. I. Friel, S. L. Clewes, H. K. Dhillon, N. Perkins, D. J. Twitchen, and G. A. Scarsbrook, Diam. Relat. Mater. **18**, 808 (2009).
2. A. A. Demidovich, A. S. Grabtchikov, V. A. Orlovich, M. B. Danailov, and W. Kiefer, in *Conference on Lasers and Electro-Optics Europe* (European Physical Society, 2005), p. 251.
3. W. Lubeigt, G. M. Bonner, J. E. Hastie, M. D. Dawson, D. Burns, and A. J. Kemp, Opt. Express **18**, 16765 (2010).
4. X. Chen, X. Zhang, Q. Wang, P. Li, S. Li, Z. Cong, G. Jia, and C. Tu, Opt. Lett. **33**, 705 (2008).
5. P. G. Zverev, T. T. Basiev, and A. M. Prokhorov, Opt. Mater. **11**, 335 (1999).
6. C. Zhang, X. Y. Zhang, Q. P. Wang, S. Z. Fan, X. H. Chen, Z. H. Cong, Z. J. Liu, Z. Zhang, H. J. Zhang, and F. F. Su, Laser Phys. Lett. **6**, 505 (2009).
7. R. P. Mildren and A. Sabella, Opt. Lett. **34**, 2811 (2009).
8. R. Loudon, Adv. Phys. **13**, 423 (1964).
9. S. A. Solin and A. K. Ramdas, Phys. Rev. B **1**, 1687 (1970).
10. A. Penzkofer, A. Laubereau, and W. Kaiser, Prog. Quantum Electron. **6**, 55 (1979).
11. N. S. Nagendra Nath, Proc. Indian Acad. Sci. A **1**, 333 (1934).
12. A. A. Kaminskii, R. J. Hemley, J. Lai, C. S. Yan, H. K. Mao, V. G. Ralchenko, H. J. Eichler, and H. Rhee, Laser Phys. Lett. **4**, 350 (2007).